Surface Expansion Is Independent of and Occurs Faster than Core Solvation during the Unfolding of Barstar[†]

K. Sridevi and Jayant B. Udgaonkar*

National Centre for Biological Sciences, Tata Institute of Fundamental Research, GKVK Campus, Bangalore 560065, India

Received September 18, 2002; Revised Manuscript Received November 20, 2002

ABSTRACT: The denaturant-induced unfolding kinetics of the 89-residue protein, barstar, have been examined using fluorescence resonance energy transfer (FRET) at 25 °C and pH 8.0. The core tryptophan, Trp53, in barstar serves as a fluorescence donor, and a thionitrobenzoic acid moiety (TNB) attached to a cysteine residue acts as an acceptor to form an efficient FRET pair. Four different single-cysteine containing mutants of barstar with cysteine residues at positions 25, 40, 62, and 82 were studied. The unfolding kinetics of the four mutant forms of barstar were monitored by measurement of the changes in the fluorescence intensity of Trp53 in the unlabeled and TNB-labeled proteins. The rate of change of fluorescence of the single-tryptophan residue, Trp53, in the unlabeled protein, where no FRET occurs, yields the rate of solvation of the core. This rate is similar for all four unlabeled proteins. The rate of the increase in the fluorescence of Trp53 in the labeled protein, where FRET from the tryptophan to the TNB label occurs, yields the rate of decrease in FRET efficiency during unfolding. The decrease in FRET efficiency for proteins labeled at either of the two buried positions (Cys40 or Cys82) occurs at a rate similar to the rate of core solvation. The decrease in FRET efficiency for the acceptor at Cys40 is also shown to be sensitive to the isomerization of the Tyr47−Pro48 *cis* bond. For the proteins where the label is at a solvent-exposed position (Cys25 and Cys62), the decrease in FRET efficiency occurs in two kinetic phases; 15−25% of the FRET efficiency decreases in the faster phase, and the remaining FRET efficiency decreases in a slower phase, the rate of which is the same as the rate of core solvation. These results clearly indicate that, during unfolding, the protein surface expands faster than, and independently of, water intrusion into the core.

Classically, all polypeptide chains are expected to fold *via* a folding pathway, which is a well-defined sequence of events that carries the protein from the unfolded, random coil-like state to the native state (*1*). The pathway concept implies that protein unfolding must follow the reverse sequence of events because each step in the folding pathway is reversible. On the other hand, the energy landscape perspective of protein folding envisions the folding reaction as representing the ensemble average of a process that is microscopically heterogeneous (*2*, *3*). Statistical models of protein folding in the energy landscape perspective suggest that unfolding may not be a direct reversal of folding (*4*). Experimentally, it has been difficult to compare folding and unfolding kinetics, because folding and unfolding experiments are carried out under different solvent conditions. Even though the same structural transitions may be involved in both folding and unfolding, the rate-limiting steps under the two experimental conditions may be different, and hence, the observable intermediate structures may be different. Thus, it is not possible to predict the unfolding kinetics of a protein, even when its folding kinetics have been thoroughly characterized.

Experimental characterization of protein unfolding kinetics became important due to the prediction that complex energy landscapes are likely to be available for unfolding (*3*, *4*) as they are for folding. Indeed, kinetic intermediates have been detected in the unfolding of ribonuclease A (*5*−*7*), myoglobin (*8*), *Escherichia coli* DHFR (*9*), and barstar (*10*−*12*). Single-molecule unfolding studies also indicate that unfolding occurs in a stepwise manner (*13*, *14*). A study of the mechanical unfolding of a β-hairpin by molecular dynamics (MD) simulations has also indicated stepwise unfolding pathways, wherein the complete breakdown of backbone hydrogen bonds precedes dissociation of the hydrophobic cluster (*15*). The relaxation kinetics of *E. coli* CspA in response to laser-induced temperature jumps indicate the existence of multiple unfolding pathways (*16*). The thermal unfolding of *E. coli* DHFR by MD simulations (*17*) indicated that the core is most resistant to unfolding, and that it unfolds after all the other domains have unfolded.

The main experimental observables in protein folding and unfolding experiments have been exponential decays of optical signals. Experimentally observed protein folding kinetics fall into two classes: multistate (*18*−*22*) and two-state kinetics (listed in ref *23*). The study of proteins which fold and unfold by two-state kinetics gives relatively little

[†] This work was funded by the Tata Institute of Fundamental Research and the Department of Science and Technology, Government of India. K.S. is the recipient of a Kanwal Rekhi Scholarship for Career Development. J.B.U. is the recipient of a Swarnajayanti Fellowship from the Government of India.

* To whom correspondence should be addressed. E-mail: jayant@ncbs.res.in. Fax: 91-80-3636662.

10.1021/bi0268697 CCC: $25.00
Published on Web 01/25/2003

information about the conformational space available to a polypeptide chain for sampling. The observation of multistate folding and unfolding kinetics allows the experimental characterization of the theoretically postulated energy landscapes, and enables the understanding of the physical interactions that play a role in the rate-limiting steps of folding and unfolding.

The detection of intermediates in protein (un)folding studies depends on the sensitivity of the method used for monitoring the structural transitions. Measurement of circular dichroism (CD) signals enables monitoring of the changes in secondary structure, while fluorescence emission is used for monitoring changes in tertiary structure. These optical signals give information only about the average properties of all forms of the protein present at the time of measurement, and they do not give residue specific information. Equilibrium or pulsed hydrogen exchange measurements give information about the status of individual residues during the unfolding transition (*7*, *24*−*26*). Exchange occurs upon solvent exposure during unfolding, whereas groups that are buried remain protected from exchange. Equilibrium and pulse labeling of cysteine thiols have also been used for characterizing unfolding transitions under both low- and high-denaturant conditions for barstar (*12*, *27*). A thiol−disulfide exchange study of apomyoglobin during its unfolding enabled the identification of the site for initial tertiary structure breakdown (*28*). Both the hydrogen exchange and thiol exchange methods suffer from the drawback that obtaining information about residues which are solvent-exposed in the native state is relatively difficult.

Fluorescence resonance energy transfer (FRET)[1] is a sensitive method for monitoring structural transitions in proteins (reviewed in refs *29* and *30*). FRET is the transfer of excited-state energy from the initially excited donor fluorophore to an acceptor fluorophore, by a radiationless process. It requires that the donor molecules emit at wavelengths which overlap with the absorption spectrum of the acceptor (*31*). The efficiency of energy transfer depends on the distance between the donor and acceptor fluorophores present in the protein. The transfer efficiency can be determined by fluorescence measurements of the extent of quenching of the donor fluorescence by the acceptor. The distance between a donor fluorophore and an acceptor located in a protein, as well as the change in this distance accompanying a structural transition, can therefore be monitored by FRET. The donor and acceptor positions can be designed appropriately for observing changes in specific intramolecular distances, involving either buried or exposed residues. Distance distributions during the equilibrium unfolding of barstar (*32*), bovine pancreatic RNase A (*33*), and cytochrome *c* (*34*) have been determined by time-resolved FRET experiments. The only instance of unfolding kinetics studied by FRET is for yeast phosphoglycerate kinase (PGK) (*35*), where the unfolding process was shown to begin by movement of the two domains of the protein away from each other. More recently, FRET has been used for monitoring the refolding kinetics of cytochrome *c* (*34*, *36*) and acyl-CoA binding protein (*37*).

[1] Abbreviations: DTNB, 5,5′-dithiobis(2-nitrobenzoic acid); FRET, fluorescence resonance energy transfer; EDTA, ethylenediaminetetraacetic acid; CD, circular dichroism.

Barstar, an 89-residue protein, has been extensively used for protein folding and unfolding studies (*10*−*12*, *18*, *27*, *32*, *38*−*41*). The folding as well as unfolding reactions of barstar appear to be multistate with discrete intermediates populating parallel pathways. The Tyr47−Pro48 bond is in the *cis* conformation in the native state, and in the unfolded state it exists in both the *cis* (U_F or the fast folding form) and *trans* (U_S or the slow folding form) conformations. Native barstar with a high denaturant concentration unfolds to U_F *via* parallel competing pathways where intermediates have been detected (*11*, *12*).

In the study presented here, a multisite FRET approach has been used for the first time to characterize structural events during the unfolding of barstar. The core tryptophan (Trp53) of barstar has been used as the donor fluorophore. An acceptor site was engineered at each of four different locations in barstar by cysteine substitution mutagenesis, followed by labeling with TNB. It is shown, from the changes in the FRET efficiency that occur during unfolding of all four proteins containing Trp53 and either Cys25-TNB, Cys40-TNB, Cys62-TNB, or Cys82-TNB, that the surface residues move away from the core faster than water penetrates into the core. The use of multiple FRET pairs has enabled measurement of specific structural changes which cannot be observed by routinely used spectroscopic methods.

MATERIALS AND METHODS

Protein Purification. Wild-type barstar contains three tryptophans (Trp38, Trp44, and Trp53) and two cysteines (Cys40 and Cys82). All the mutant versions of barstar used in this study contain a single tryptophan residue (Trp53) and a single cysteine at one of four different locations. For simplicity, the mutant proteins are denoted by the position of the single cysteine residue present in them. The mutant proteins W38F/W44F/S12T/C40A (Cys82), W38F/W44F/C82A (Cys40), W38F/W44F/C40A/C82A/A25C (Cys25), and W38F/W44F/C40A/C82A/L62C (Cys62) were generated by site-directed mutagenesis, and the proteins were purified as described previously (*42*). Protein concentrations were determined by absorbance at 280 nm, using an ϵ_{280} of 10 000 M^{-1} cm^{-1} (*43*) for all the proteins. Mass spectrometry on a Micromass Q-TOF Ultima instrument showed that the masses of the different mutant forms of barstar were 10 232 Da for Cys25 and Cys40, 10 190 Da for Cys62, and 10 246 Da for Cys82. Each mass is consistent with the N-terminal methionine remaining uncleaved. The TNB-labeled proteins were obtained by reaction of the protein in 8 M urea (pH 8.5) with a 100-fold molar excess of DTNB (*44*). After the labeling reaction was complete, the free dye and urea were removed by passing the protein through a PD10 column (Pharmacia). Mass spectrometric characterization showed that all proteins were >98% labeled, with the expected 196 Da increase in mass due to the TNB group.

Buffers and Solutions. All experiments were carried out at 25 °C, in buffer containing 20 mM Tris and 0.25 mM EDTA (pH 8.0). Concentrations of stock urea solutions were determined by refractive index measurements. In all the experiments, the protein concentration that was used was 15−20 μM.

Measurement of Absorption Spectra. The absorption spectra of the TNB-labeled proteins were collected on a CARY100 double-beam spectrophotometer. The spectra were

collected with a bandwidth of 1 nm and a scan speed of 1 nm/s, using a cuvette with a path length of 1 cm.

Measurement of Equilibrium Unfolding Transitions. For equilibrium unfolding measurements, barstar solutions containing different concentrations of denaturant were incubated for ~3 h (incubation periods ranging from 2 to 24 h gave the same results). Tryptophan fluorescence excited at 295 nm was monitored at 320 and 380 nm for the unlabeled protein, and at 380 nm for the TNB-labeled proteins, using the MOS-250 detection system. Circular dichroism (CD) measurements were taken on a Jasco 720 spectropolarimeter, as described previously (*41*).

Measurement of Unfolding Rates by Fluorescence. Unfolding reactions with different urea concentrations were carried out in the stopped-flow module (SFM 400). 40 μL of the native protein (~100 μM) was diluted into different urea concentrations to a final volume of 300 μL. The mixing dead time for the reactions was 4.1 ms. Fluorescence changes during the unfolding kinetics were monitored at 320 nm for the unlabeled proteins (donor alone sample), and at 380 nm for the TNB-labeled proteins (donor−acceptor sample) upon excitation at 295 nm, using the MOS-250 detection system.

DATA ANALYSIS

Analysis of Equilibrium Unfolding Transitions. Measurements of fluorescence intensity or CD at different urea concentrations were analyzed according to a two-state, N ⇌ U, mechanism (*45*) to determine the free energy change for unfolding [$\Delta G_U(H_2O)$] and the midpoint of the unfolding transition (C_m).

Analysis of Fluorescence-Monitored Kinetics. At each denaturant concentration, the change in fluorescence intensity (y) observed for the unfolding reactions as a function of time t at different denaturant concentrations was fit to either a single- or two-exponential equation, given by

$$y = y_0 + a^{-\lambda_1 t} \tag{1a}$$

$$y = y_0 + a^{-\lambda_1 t} + b^{-\lambda_2 t} \tag{1b}$$

where y_0 is the fluorescence intensity when the reaction is complete (t = infinity), λ_1 and λ_2 are the apparent rate constants, and a and b are the amplitudes of the kinetic phases.

Analysis of FRET. The efficiency of energy transfer for a donor−acceptor pair depends on the distance R between the donor and acceptor and is given by Forster's relation (*31*):

$$E = \left(1 + \frac{R^6}{R_0^6}\right)^{-1} \tag{2a}$$

$$R_0 = 0.211(\kappa^2 n^{-4} Q_D J]^{1/6}\ (\text{Å}) \tag{2b}$$

$$J = \frac{\int F(\lambda)\, \epsilon(\lambda)\, \lambda^4\, d\lambda}{\int F(\lambda)\, d\lambda}\ (\text{M}^{-1}\,\text{cm}^{-1}\,(\text{nm})^4) \tag{2c}$$

where R_0 is the Forster's distance, J is the overlap integral, Q_D is the quantum yield of the donor, n is the refractive index of the medium, and κ^2 is the orientation factor (*31*).

For the determination of J, the fluorescence emission spectra [$F(\lambda)$] of the unlabeled proteins were collected on the SFM 400 coupled to the MOS-250 detection system, using an excitation wavelength of 295 nm (bandwidth of 5 nm) and measuring emission from 310 to 410 nm (bandwidth of 10 nm). Absorption spectra for the TNB-labeled proteins were collected as described above, from 310 to 410 nm. All absorption spectra were divided by the respective protein concentration (in molar) to obtain $\epsilon(\lambda)$. J was determined as the overlap between $F(\lambda)$ and $\epsilon(\lambda)$ according to eq 2c, where the wavelength λ is in nanometers (*31*).

For the determination of the Q_D values of the N and U forms, use was made of the previously published value for Trp of 0.14 (*46*). Under similar conditions, the fluorescence lifetime of Trp is 2.6 ns and that of the N state of the barstar is 4.97 ns (*32*). Since Q_D is proportional to the fluorescence lifetime, the Q_D of the N state was determined to be 0.27 (*32*). Using this value for the Q_D of the N state, and the ratio of the area under the fluorescence spectrum of U to the area under the fluorescence spectrum of N, the Q_D of the U state was determined to be 0.11.

The fluorescence intensities of the donor−acceptor samples (F_{DA}) and of the donor-alone sample (F_D) can be used to determine the energy transfer efficiency:

$$E = 1 - \frac{F_{DA}}{F_D} \tag{2d}$$

The change in energy transfer efficiency during an unfolding reaction, that is, during a transition from the native (N) state to the unfolded (U) form of the protein, is given as

$$\Delta E_{N-U} = \left(1 - \frac{F_{DA,N}}{F_{D,N}}\right) - \left(1 - \frac{F_{DA,U}}{F_{D,U}}\right) \tag{3a}$$

where the subscripts N and U refer to the properties of the native and unfolded proteins, respectively. If the donor fluorescence in the native and unfolded proteins are similar, that is, $F_{D,N} = F_{D,U} = F_D$, then

$$\Delta E_{N-U} = \frac{F_{DA,N} - F_{DA,U}}{F_D} = \frac{\Delta F_{DA}}{F_D} \tag{3b}$$

Thus, the change in the fluorescence of the donor−acceptor sample during unfolding represents directly the change in the energy transfer efficiency between the donor and acceptor during unfolding.

RESULTS

Quenching of Fluorescence of the TNB-Labeled Proteins Is Due to FRET. Figure 1 shows Trp53 and the position of the cysteine residue in each of the four different single-cysteine containing mutants of barstar. The fluorescence emission spectrum is identical in shape and intensity for all four mutant proteins studied here (data only for Cys25 and Cys40 are shown in panels a and b of Figure 2). The fluorescence of both native and unfolded forms is quenched upon labeling the cysteine with TNB, as seen from the spectra of Cys25-TNB and Cys40-TNB in panels a and b of Figure 2. The shapes of the fluorescence spectra remain the same, and only the fluorescence intensity is reduced upon TNB labeling. The spectra of the two labeled proteins shown

Table 1: Energy Transfer Parameters

FRET pair	solvent accessibility of Cys (%)[a]	FRET efficiency		J^* ($\times 10^{-13}$ M^{-1} cm^{-1} nm^4)		R_0 (Å)[b]		D−A distance in N (Å)	
		N	U	N	U	N	U	by FRET	calcd[c]
Trp53−Cys25	54	0.84	0.46	7.4	7.6	26.9	22.5	20.4	17.0
Trp53−Cys40	5	0.92	0.61	5.1	7.8	25.2	22.6	16.8	16.8
Trp53−Cys62	42	0.95	0.69	7.3	8.2	26.8	22.6	16.4	11.6
Trp53−Cys82	20	0.96	0.33	7.7	8.1	27.0	22.7	15.9	16.9

[a] Percent accessible surface area, calculated in comparison with a model tripeptide (*59*). [b] R_0 was calculated using eq 2b, using the following values: $\kappa^2 = {}^2/_3$, $n = 1.33$ for N and 1.4 for U, and $Q_D = 0.27$ for N and 0.11 for U. J was calculated using eq 2c. [c] An average coordinate was calculated for the side chain of each residue from the coordinates in PDB entry 1bta, and the average distance between any two residues from these coordinates was estimated. The coordinates for all atoms in the side chain were considered for calculating the average coordinate.

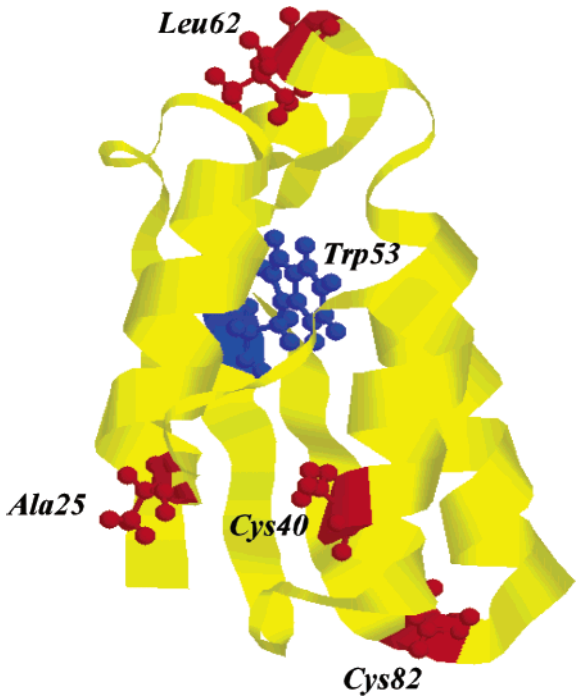

FIGURE 1: NMR structure of barstar (generated by RASMOL using PDB entry 1bta) indicating the positions of the single tryptophan (Trp53) and the single cysteine residues (Cys25, -40, -62, and -82) in the mutant proteins used for the unfolding experiments.

in panels a and b of Figure 2 indicate that (i) the extent of quenching depends on the position of the TNB label and (ii) the extent of quenching in the native state is far greater than that seen in the unfolded form. The observation that the extent of quenching depends on the distance between Trp53 and the Cys-TNB, and it is more in the compact native state compared to the expanded unfolded form, indicates that the quenching is due to FRET between the donor (Trp53) and the acceptor (TNB).

The energy transfer efficiency can be determined using eq 2d, by measuring the fluorescence of the donor in the absence of acceptor F_D (in the unlabeled protein), and of the donor in the presence of acceptor F_{DA} (in the corresponding TNB-labeled protein). The energy transfer efficiency (E) for each of the four FRET pairs, in the native (N) as well as unfolded (U) form, was determined using the total area under the fluorescence spectrum (310 nm − 410 nm) for F_D as well as for F_{DA} (Table 1). E can be used to determine the distance R between the donor and acceptor using eq 2a. This requires determination of R_0, as given by eq 2b. The overlap integral (J) was determined for each donor−acceptor pair. The quantum yield of Trp53 in the native state of Cys82 mutant of barstar had earlier been determined to be 0.27 (*32*). The orientation factor κ^2 depends on how Trp53 and the TNB moeity are oriented with respect to each other. If the donor and acceptor are oriented randomly with respect to each other, the value of κ^2 is ${}^2/_3$ (*47*, *48*). The donor, Trp53, and a fluorescent label attached to Cys82 have been shown to have sufficient motional freedom by time-resolved fluorescence anisotropy measurements (*32*, *49*), and the assumption of a random orientation of the donor and acceptor in the native state was justified previously (*32*) for the Trp53−Cys82-TNB pair. Apart from this FRET pair, three other FRET pairs have been used for this study, but all of these have a common donor (Trp53). The donor properties as seen from the shape of the fluorescence emission spectra and fluorescence lifetime decays (data not shown) are identical in all four mutant proteins. Thus, the quantum yield and the motional freedom of the donor are assumed to be the same in all the mutants studied here. Cys82 is a buried residue, and it was shown that a fluorescent probe attached to it has significant rotational freedom. It is therefore reasonable to assume that the other buried cysteine residue, Cys40, and the exposed Cys residues (Cys25 and -62; see below) have similar rotational freedom. Thus, the assumption of a value of ${}^2/_3$ for κ^2 was made for the calculation of R_0 for all the FRET pairs (Table 1). Estimates of distances made with this assumption are found to match estimates using other methods for other proteins (*50*). The distances in the native state recovered from FRET analysis (Table 1) agree reasonably with the distances calculated from the NMR structure (*51*) of barstar. It should be noted that the energy transfer efficiency, and hence the distance, can be determined more accurately by measurement of the fluorescence lifetimes of the donor alone and donor−acceptor samples.

Cys25 and Cys62 Are Solvent-Exposed. Calculation of the degree of solvent exposure of various residues from the NMR structure of barstar (Figure 1 and Table 1) indicates that residues 40 and 82 are buried and residues 25 and 62 are solvent-exposed. The absorption spectrum of the TNB group is environment sensitive; the absorption maximum is red-shifted upon solvent exposure. Figure 2c shows the absorption spectra of Cys25-TNB in the native and unfolded forms. The coincidence of the two spectra, with absorption maxima at 336 nm, indicates that the TNB group is as solvent-exposed in the native state as it is in the fully unfolded form. Figure 2d shows the absorption spectra of Cys40-TNB in the native and unfolded forms. The absorption maximum of the native protein at 320 nm is clearly blue-shifted with respect to the absorption maximum of the unfolded protein at 336 nm. This indicates that the TNB attached to Cys40 is buried in the native state and becomes solvent-exposed upon unfolding. The absorption maxima of Cys62-TNB and

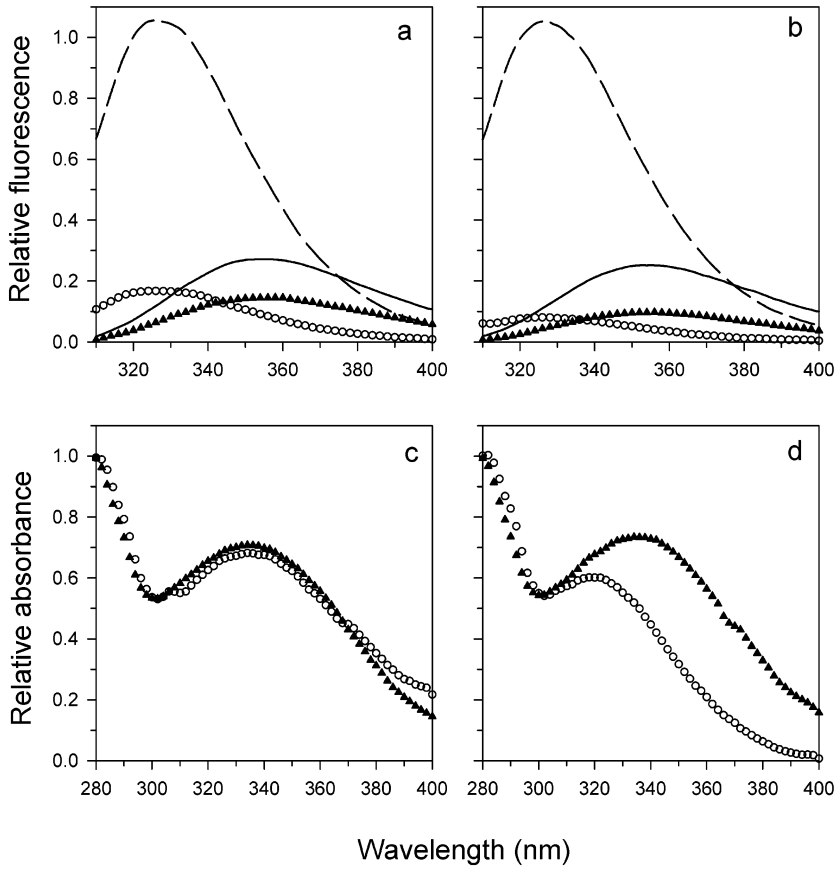

FIGURE 2: Fluorescence and absorption spectra of unlabeled and TNB-labeled Cys25 (a and c) and Cys40 (b and d). (a and b) Fluorescence spectra of unlabeled proteins in the native state (– – –) and the unfolded form (—) and the TNB-labeled protein in the native (○) and unfolded (▲) forms. All fluorescence spectra are normalized to a value of 1 for the fluorescence intensity at 320 nm for the native, unlabeled Cys25 protein. The excitation wavelength was 295 nm with a 5 nm bandwidth, and the emission bandwidth was 20 nm. (b and d) Absorption spectra of the TNB-labeled proteins in the native (○) and unfolded (▲) forms. Absorption spectra were collected with a 1 nm bandwidth.

Cys82-TNB in the unfolded forms are also at 336 nm. The absorption maximum of native Cys62-TNB is at 330 nm, and that of native Cys82-TNB is at 326 nm (data not shown).

The extent of solvent exposure in the native state can also be deduced from the kinetics of labeling of the cysteine residue with DTNB (*27*). A solvent-exposed cysteine residue is expected to be labeled at similar rates in the native and unfolded forms. Cys82 and Cys40 label at a much slower rate in the native state than in the unfolded state (*12*, *27*), because they are buried residues. Although the absorption maximum of native Cys62-TNB is blue-shifted relative to the completely exposed TNB absorption maximum, it was seen that native Cys62 is labeled at a fast rate comparable to the labeling rate in the completely unfolded protein (data not shown). Native Cys25 too is labeled at the same rate as is unfolded Cys25. Thus, the TNB absorption maxima and the cysteine labeling kinetics indicate that the TNB group is solvent-exposed when attached to Cys25 or Cys62, while it is buried when attached to Cys40 or Cys82.

TNB Labeling Does Not Alter Stability. Figure 3a shows that the urea-induced equilibrium unfolding transitions of Cys25 and Cys25-TNB proteins monitored by mean residue ellipticity at 222 nm are coincident, indicating that TNB labeling does not alter the stability of the protein. The values of $\Delta G_U(H_2O)$ and C_m for the unfolding transition were determined from two-state analysis of the unfolding transition, for all the TNB-labeled and unlabeled proteins, and are given in Table 2. The stabilities of the different mutant proteins are similar, and are not significantly altered upon labeling. The only exception is Cys40, the stability of which increases upon labeling with TNB, as reported previously (*44*).

Table 2: Stability Parameters Calculated from Urea-Induced Equilibrium Unfolding Transitions

protein	ΔG_U (kcal/mol)	C_m (M)	protein	ΔG_U (kcal/mol)	C_m (M)
Cys25	-4.4 ± 0.5	3.5 ± 0.1	Cys25-TNB	-4.3 ± 0.5	3.4 ± 0.1
Cys40	-4.2 ± 0.5	3.3 ± 0.1	Cys40-TNB	-4.7 ± 0.5	3.7 ± 0.1
Cys62	-4.0 ± 0.5	3.3 ± 0.1	Cys62-TNB	-4.1 ± 0.5	3.4 ± 0.1
Cys82	-4.5 ± 0.5	3.4 ± 0.1	Cys82-TNB	-4.5 ± 0.5	3.5 ± 0.1

The equilibrium unfolding transition can also be monitored by measurement of the change in the fluorescence intensity of Trp53. Figure 3b shows the equilibrium unfolding transition of Cys25 monitored by fluorescence at 320 nm. The difference in the fluorescence spectra of the native and unfolded forms of Cys25 is maximal at 320 nm, so this wavelength was chosen for observation of the unfolding transition. On the other hand, the difference between the fluorescence of the native and unfolded forms of Cys25 is smallest at 380 nm (Figure 3b, inset). This indicates that the fluorescence of Trp53 at 380 nm does not change significantly in response to the change in its environment upon unfolding. To monitor the change in FRET efficiency during unfolding, the changes in the fluorescence of the donor alone (F_D) and donor−acceptor (F_{DA}) proteins have to be monitored (eq 2d). If during the unfolding process the change in

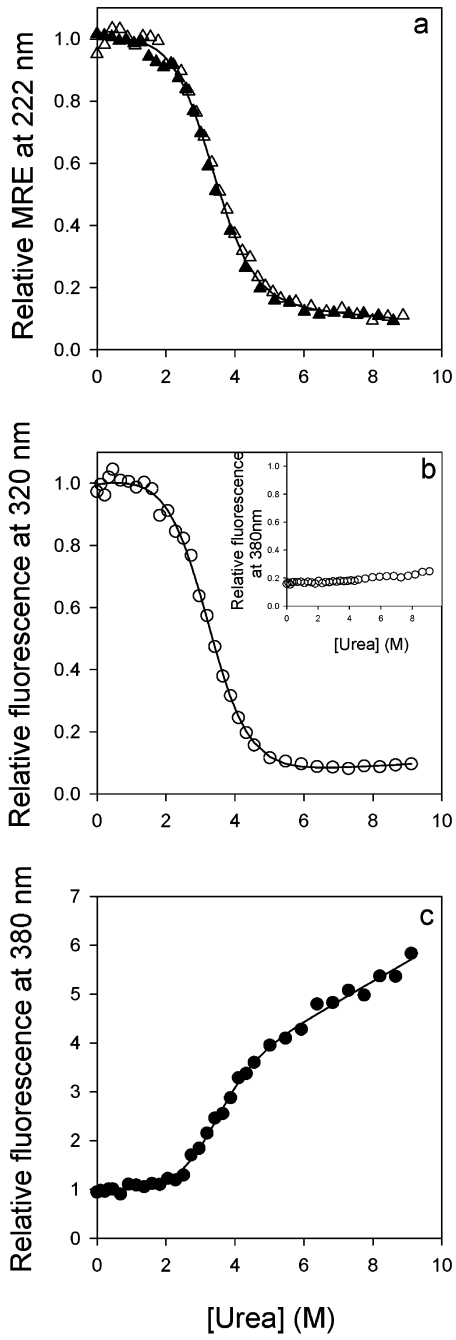

FIGURE 3: Equilibrium unfolding transitions of Cys25 and Cys25-TNB. (a) Equilibrium unfolding transitions monitored by mean residue ellipticity at 222 nm for Cys25 (△) and Cys-TNB (▲). The lines through the data are fits obtained by two-state analysis. (b) Equilibrium unfolding transition of Cys25 monitored by fluorescence emission at 320 and 380 nm (inset). The fluorescence intensities at both wavelengths are normalized to the fluorescence intensity of the native protein at 320 nm. (c) Equilibrium unfolding transition of Cys25-TNB monitored by fluorescence emission at 380 nm. The fluorescence intensity is normalized to the fluorescence intensity of the native protein at 380 nm. The excitation wavelength for all measurements was 295 nm.

the donor fluorescence is negligible, then the observed fluorescence-monitored unfolding kinetics of the donor−acceptor samples (F_{DA}) represent directly the kinetics of change of the energy transfer efficiency (E) between the donor and acceptor (eqs 3a and 3b). Since at 380 nm the change in the donor fluorescence (F_D) is negligible, the fluorescence of the TNB-labeled proteins (F_{DA}) was monitored at 380 nm, to simplify the FRET analysis. Figure 3c shows the equilibrium unfolding transition of Cys25-TNB monitored at 380 nm. Two-state analysis of the equilibrium unfolding transitions monitored by fluorescence emission gave values for $\Delta G_U(H_2O)$ and C_m similar to those obtained from the analysis of unfolding transitions monitored by CD. Also, the unfolding transition of Cys25-TNB monitored by fluorescence emission at 320 nm gives the same stability. In principle, the FRET experiments can be carried out at any wavelength. In this study, FRET was monitored at 380 nm, which allows the simplifying assumption, as described above, to be made in the FRET analysis.

Complete Unfolding Kinetics Can Be Observed for Labeled and Unlabeled Proteins. A representative trace of the fluorescence-monitored unfolding kinetics for Cys82 (in 7 M urea) is shown in Figure 4a. The decrease in fluorescence intensity at 320 nm during unfolding of Cys82 occurs in a single phase which can be fit to eq 1a. The inset in Figure 4a shows the goodness of the single-exponential fit to the first 200 ms of unfolding data. Figure 4b shows the unfolding kinetics of Cys82-TNB (in 6.5 M urea). The increase in fluorescence intensity at 380 nm due to the decrease in FRET during unfolding also occurs in a single kinetic phase. The start and end points of the unfolding kinetics match the expected amplitude of the complete unfolding reaction observed in the equilibrium unfolding transition for both the unlabeled and TNB-labeled proteins (Figure 4c,d).The entire unfolding kinetics for the other three mutant proteins and their TNB-labeled forms are also observable (Figures 5a,b and 6) and consistent with the amplitudes expected from their equilibrium unfolding transitions (data not shown).

Unfolding Kinetics Monitored by FRET for the Buried Residues (Cys40 and Cys82). The unfolding kinetics of Cys82 and Cys82-TNB are very similar as seen from the good agreement in the apparent rates of unfolding of the two proteins at different urea concentrations (Figure 4e). The unfolding kinetics of Cys40 and Cys40-TNB are shown in Figure 5. The representative unfolding kinetic trace for Cys40 shown in Figure 5a (in 7.1 M urea) indicates that the fluorescence change upon unfolding occurs in a single phase with a rate constant of $\sim$1 s^{-1}. Figure 5b shows a representative unfolding kinetic trace of Cys40-TNB (in 7.1 M urea). There are clearly two kinetic phases with apparent rates of $\sim$0.35 and $\sim$0.027 s^{-1} . The observed unfolding rates for Cys40 and Cys40-TNB obtained by fitting the kinetic data to eq 1a or 1b are compared in Figure 5c. The observed unfolding rate for Cys40 is greater than the faster unfolding rate observed for Cys40-TNB. The slower unfolding rates for both Cys40 and Cys40-TNB are similar in magnitude in the urea concentration range where both can be measured. Figure 5d shows the relative amplitude of the faster of the two unfolding phases observed for Cys40-TNB. At higher urea concentrations, where only Cys40-TNB shows a measurable unfolding rate, the rate and its relative amplitude are invariant with urea concentration.

Unfolding Kinetics Monitored by FRET for the Solvent-Exposed Residues (Cys25 and Cys62). Panels a and b of Figure 6 show representative unfolding kinetic traces for Cys25 and Cys62. The unfolding kinetics of Cys25 as well as of Cys62 are described well by a single-exponential phase that accounts for the entire expected unfolding amplitude.

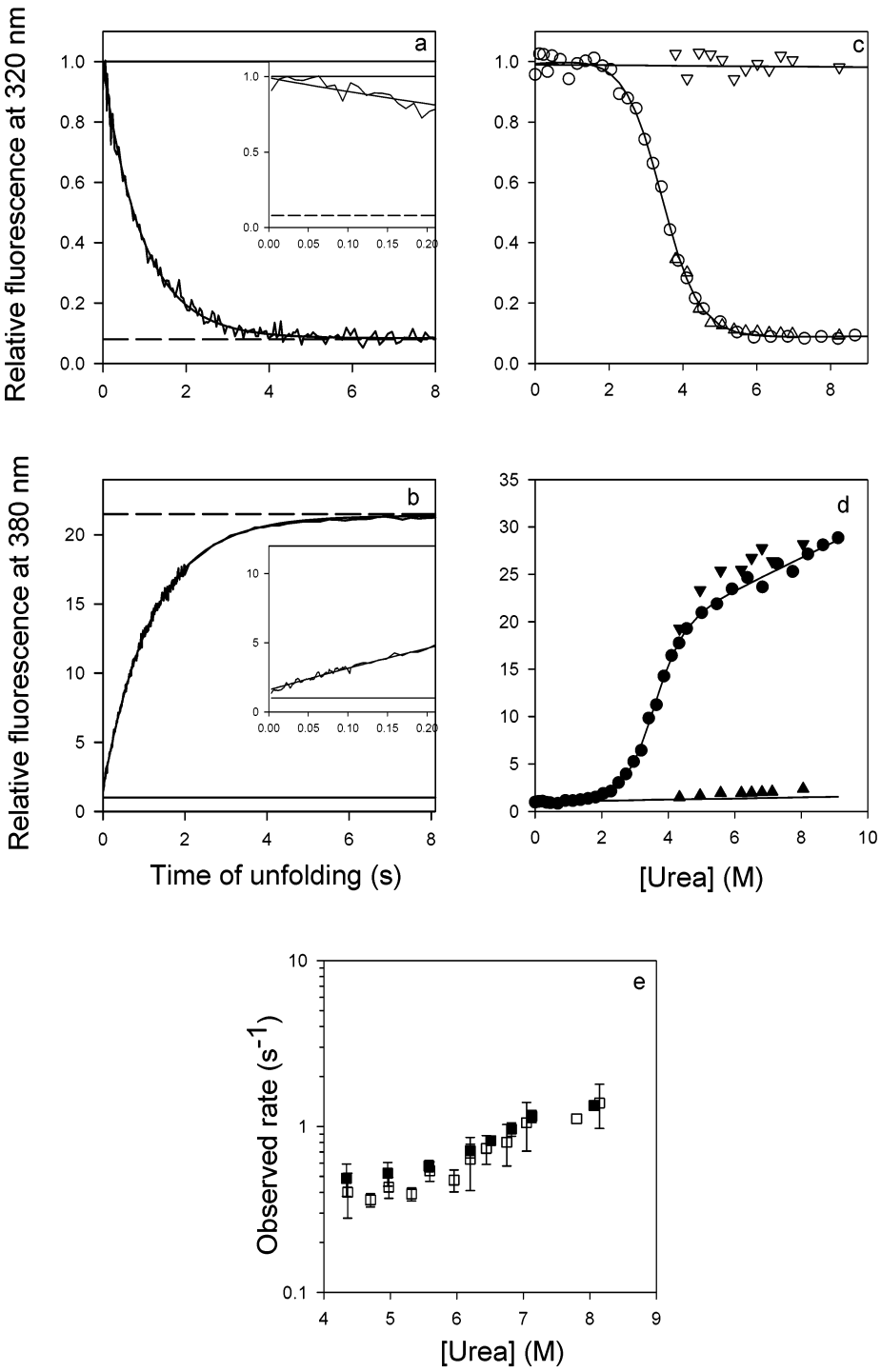

FIGURE 4: Unfolding kinetics of Cys82 and Cys82-TNB. (a and b) Representative unfolding kinetic traces monitored by fluorescence emission at 320 nm for Cys82 unfolding in 7.0 M urea (a) and at 380 nm for Cys82-TNB unfolding in 6.5 M urea (b). The insets show the unfolding traces during the first 200 ms. The data are normalized to the fluorescence of the respective native protein. The lines through the data in panels a and b represent fits to eq 1a (Materials and Methods). The native (—) and unfolded (– – –) signals expected from the equilibrium unfolding transition are also shown. Panels c and d show the equilibrium unfolding transitions (○ and ●, respectively) and the start (△ and ▲, respectively) and end points (▽ and ▼, respectively) of the kinetic unfolding experiments for Cys82 (c) and Cys82-TNB (d). (e) Observed unfolding rates obtained by fitting the fluorescence-monitored kinetics to eq 1a, for Cys82 (□) and Cys82-TNB (■).

The insets in panels a and b of Figure 6 show that the data fits are well described by single-exponential kinetics at short unfolding times. Panels c and d of Figure 6, which show representative kinetic traces for Cys25-TNB and Cys62-TNB, clearly indicate that it is necessary to fit the observed kinetics to a two-exponential equation; the single-exponential fits do not pass through the data at short unfolding times. The need to use two-exponential fits is evident from the residuals of the fits of the data to single- and two-exponential equations (insets of panels c and d of Figure 6).

Thus, the unfolding kinetics of both Cys25-TNB and Cys62-TNB show an additional very fast unfolding phase not seen for the corresponding unlabeled proteins. Panels a and b of Figure 7 show the observed unfolding rates for

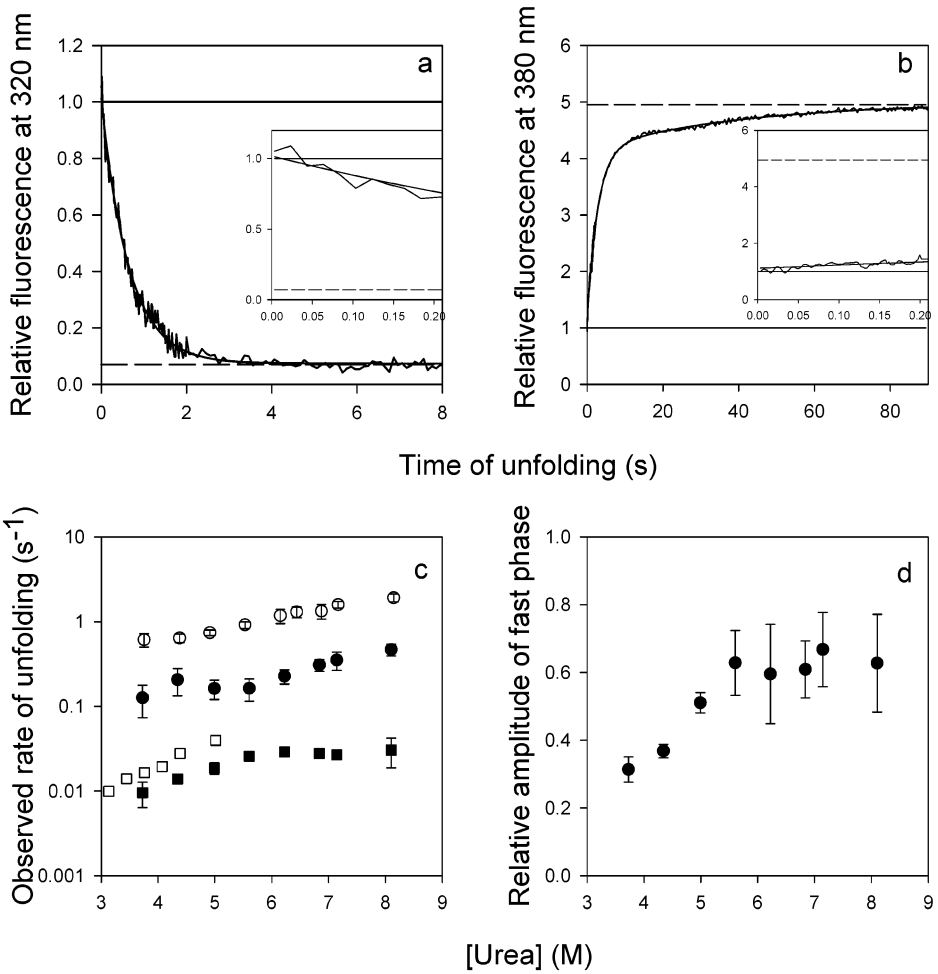

FIGURE 5: Unfolding kinetics of Cys40 and Cys40-TNB in 7.1 M urea. (a and b) Representative unfolding kinetic traces monitored by fluorescence emission at 320 nm for Cys40 (a) and at 380 nm for Cys40-TNB (b). The insets show the unfolding trace during the first 200 ms. The data were normalized to the fluorescence of the respective native protein (=1). The solid line through the data in panel a is a fit to eq 1a and in panel b is a fit to eq 1b. The native (—) and unfolded (– – –) signals expected from the equilibrium unfolding transition are also shown. (c) Observed unfolding rates for Cys40 (○ and □) and Cys40-TNB (● and ■) obtained by fitting the kinetic data to either eq 1a or 1b. (d) Relative amplitude of the fast unfolding phase for Cys40-TNB.

unlabeled and TNB-labeled Cys25 and Cys62. The fast unfolding rates of the unlabeled and TNB-labeled proteins are identical, and the TNB-labeled proteins show an additional very fast unfolding rate. The amplitude of the very fast unfolding rate is independent of urea concentration as shown in panels c and d of Figure 7.

DISCUSSION

Kinetics of Core Solvation. During unfolding, the decrease in the fluorescence intensity of the core tryptophan, Trp53, reflects a change in its environment from a hydrophobic to a solvated one, following the penetration of water into the core (*43*). The rate of fluorescence change can be interpreted directly as the rate of core solvation, because the fluorescence emission upon excitation at 295 nm is only due to the single tryptophan residue. In all the mutants studied here, the unfolding kinetics monitored by changes in the fluorescence of the core tryptophan in the unlabeled proteins are similar; the kinetics are single-exponential, and the entire fluorescence change is observable. The observed unfolding rates for all the proteins are also similar. In earlier unfolding kinetic experiments with the single-tryptophan mutant of barstar, W38F/W44F, which also contains only Trp53, a burst phase change in the fluorescence emission was reported to occur during unfolding at high urea concentrations (*11*). The absence of a burst phase change in fluorescence during unfolding, for any of the four mutant proteins used in this study, was therefore surprising, because each of these mutant proteins also contains only Trp53. The unfolding kinetics of W38F/W44F were therefore studied again, and it was seen that a burst phase change in fluorescence was absent for that mutant protein also (unpublished observations; see the Supporting Information). At present, it is unclear why the burst phase change in fluorescence was seen in the previous study, but it was likely because the protein sample was different at that time.

FRET as a Structural Probe for Monitoring Unfolding Kinetics. FRET between two residues in a protein provides site specific information in terms of the distance between the two residues, and how the two residues move with respect to each other during a structural transition. Further, if multiple FRET pairs spanning different distances in the protein are used, a more detailed picture of the structural transitions can be obtained. The unfolding transition of barstar has been studied here using four FRET pairs. The donor (Trp53) is located centrally in the hydrophobic core of the protein (*51*), and the acceptors were placed in different structural elements of barstar in four different mutant proteins: Cys25 in helix

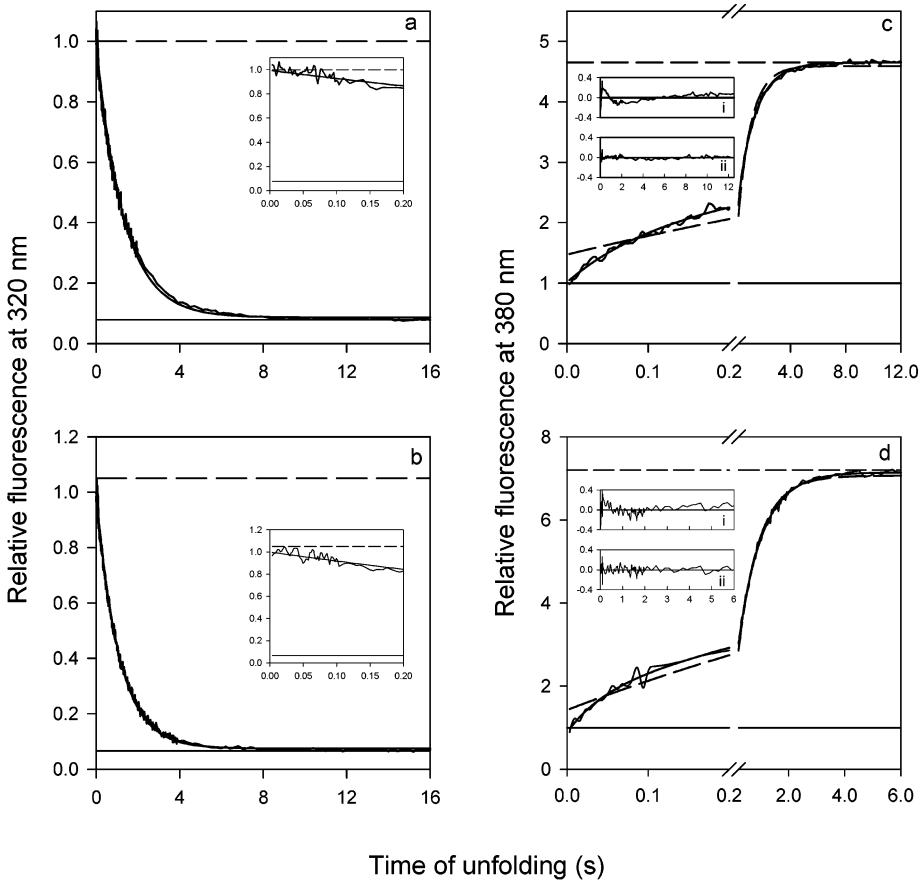

FIGURE 6: Unfolding kinetics of Cys25, Cys25-TNB, Cys62, and Cys62-TNB in 6.1 M urea. (a and b) Representative unfolding kinetic traces monitored by fluorescence emission at 320 nm for Cys25 (a) and Cys62 (b). The insets show the unfolding traces during the first 200 ms. The solid lines through the data are fits to eq 1a. (c and d) Representative unfolding kinetic traces monitored by fluorescence emission at 380 nm for Cys25-TNB (c) and Cys62-TNB (d). The solid lines through the data are fits to eq 1b, and the dashed line is a fit to eq 1a. Insets i and ii show the residuals for fits of the data to eqs 1a and 1b, respectively. All the unfolding kinetic traces are normalized to the fluorescence of the respective native protein (=1). The native (—) and unfolded (— — —) signals expected from the equilibrium unfolding transition are also shown.

1, Cys40 in helix 2, Cys62 in helix 3, and Cys82 in loop 6 (see Figure 1). These different distances allow the structural changes at these sites during the unfolding transition to be monitored. The stabilities of these mutant proteins are very similar (Table 2). Also, their fluorescence and CD spectra are identical. The stability is not significantly altered upon labeling with the acceptor (TNB), and neither the shape of the fluorescence nor the CD spectrum is altered. It is therefore reasonable to compare directly the unfolding kinetics of the four different proteins, labeled as well as unlabeled.

The energy transfer efficiency is very high for all the FRET pairs in the native states of the four proteins (Table 1), as expected for compact structures. The efficiency of energy transfer is lower in the unfolded state (U); some energy transfer is seen because the U state is not an outstretched polymer but a highly expanded random coil (*52*). The energy transfer efficiencies in the N state of each protein are well-correlated with the expected distance of the single Cys residues from Trp53, as obtained from the NMR structure (Figure 1 and Table 1). The changes in FRET efficiency accompanying the transition from the N state to the U form are large for all four FRET pairs, making measurement of FRET of each of these pairs a suitable probe for monitoring the unfolding transition of barstar.

FRET-Monitored Kinetics. The unfolding kinetics of the four TNB-labeled proteins were monitored by changes in fluorescence intensity at 380 nm. Since the change in the donor fluorescence intensity in the unlabeled protein is negligible at 380 nm (see the Results), the fluorescence change observed during unfolding for the labeled protein can be attributed directly to the change in the energy transfer efficiency (E), which accompanies unfolding. Energy transfer efficiency depends on the distance R between the donor and acceptor and the Forster's distance, R_0 (eqns 2a and 2b). R_0 depends on the orientation factor, refractive index, donor quantum yield, and overlap integral between the donor and the acceptor.

It is important to consider how R_0 might change upon unfolding from the N to U form. (i) Since the relative orientation of the donor and acceptor can be assumed to be random in the N state (see the Results), and is expected to be random in the unstructured U form, the value of the orientation factor can be assumed to be unchanged upon unfolding. (ii) The refractive index of the solvent changes from 1.33 to 1.4 upon going from native to high-denaturant conditions. (iii) The overlap integral changes only slightly from the N to the U form, and was determined for the N and U forms of all four proteins (Table 1). (iv) The quantum yield of the donor changes from 0.27 in the N state (*32*) to

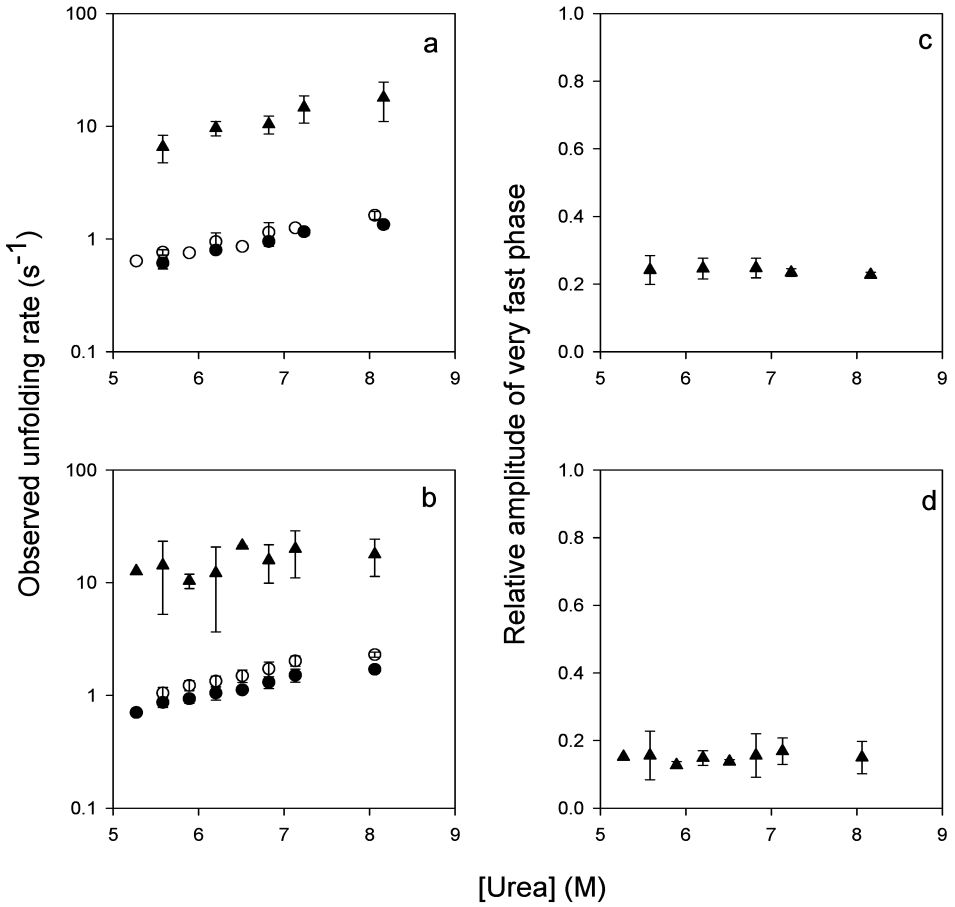

FIGURE 7: Dependence of the unfolding kinetics of Cys25 and Cys62 on urea concentration. Unfolding kinetics were monitored by tryptophan fluorescence in unlabeled proteins and by FRET in the labeled proteins. (a) Observed unfolding rates for Cys25 (○) and Cys25-TNB (● and ▲). (b) Observed unfolding rates for Cys62 (○) and Cys62-TNB (● and ▲). (c and d) Relative amplitude of the very fast phase observed for Cys25-TNB (c) and Cys62-TNB (d).

0.11 in the U form. Taking all these factors into consideration, R_0 was calculated for the N and U forms of the proteins (Table 1). If only factors i−iii above are taken into account, then the change in R_0, upon unfolding from the N to the U form, is calculated to be only 2−4%. If it is assumed that R remains the same (as in the N state), the change in E due to the change in R_0 alone would be 1−3%. When the large change in the quantum yield of the donor (Q_d), upon unfolding from the N to U form, is, however, taken into account, a large difference between the values of R_0 in the N and U forms is observed. From the values of R_0 in the N and U forms, and if the value of R in the N state (given in Table 1) were not to change, E would be expected to change by 23, 7, 8, and 7%, upon complete unfolding, for the Cys25, Cys40, Cys62, and Cys82 proteins, respectively. The observed change in E upon unfolding of the N to the U state is, however, significantly more than what is expected from a change in R_0 alone (Table 1). Thus, the change in E upon unfolding from the N to the U form must reflect, to a large extent, the change in the distance R between the donor and acceptor.

Since the change in R_0 during unfolding is primarily due to the change in the quantum yield of the donor, R_0 is expected to change significantly only in those steps of the unfolding reaction where the donor quantum yield also changes. All the four proteins have the same donor, and it is reasonable to assume, for all four proteins, that the change in R_0 occurs at the same rate as that of the change in the donor quantum yield. The unfolding kinetics of unlabeled (donor alone) proteins measure directly the kinetics of change in the quantum yield of the donor due to unfolding. If the FRET-monitored kinetics of unfolding of a labeled protein show an additional faster kinetic phase, apart from the kinetic phase also observed for the corresponding unlabeled protein, then the additional FRET-monitored kinetic phase must be a consequence of a change in the donor−acceptor distance (R) during unfolding.

FRET-Monitored Kinetics for the Solvent-Exposed Acceptors. The TNB group attached to Cys25 or Cys62 is solvent-exposed, because these residues are on the surface of the protein. Loss of FRET for the Trp53−Cys25-TNB and Trp53−Cys62-TNB pairs occurs in two kinetic phases. The faster phase (∼10−15 s^{-1}) corresponds to an ∼25% decrease in FRET efficiency for the Trp53−Cys25-TNB pair and an ∼15% decrease for the Trp53−Cys62-TNB pair. For each of these labeled proteins, the rate of the slower phase is the same as the rate of fluorescence change observed during the unfolding of the corresponding unlabeled protein. Such biphasic kinetics could imply that (1) all molecules initially expand fast to such an extent as to cause the 15−25% loss of FRET efficiency or (2) a fraction of the molecules are expanding to such an extent that the overall change in FRET that can be observed for the bulk sample is ∼20%. Situation 2 implies that some molecules are less stable and progress faster toward the unfolded state. Although there is no evidence for multiple native forms of barstar,

there is evidence for multiple unfolding pathways (*11*, *12*). The observation that the relative amplitude of the very fast unfolding phase is independent of denaturant concentration for the unfolding of both the Cys25-TNB and Cys62-TNB proteins suggests that explanation 2 is unlikely because a change in denaturant concentration might be expected to alter the distribution of molecules unfolding along one pathway or the other. Thus, it appears that all the protein molecules expand in the fast phase, leading to a partial loss of FRET efficiency. The remaining loss of FRET efficiency for all molecules occurs at the same rate as core solvation, which is the rate of the overall unfolding of the protein.

The rate of core solvation is 1 order of magnitude slower than the rate at which the partial loss of FRET efficiency between the core tryptophan and the surface residues (25 and 62) occurs, which suggests that the surface expansion occurs faster than core solvation. It appears that the surface residues of the protein move away from the core faster, and that the core slowly becomes solvated simultaneously. Using the values of *E* for the N and U states (Table 1), it can be shown that the 25% loss of FRET efficiency for Cys25-TNB corresponds to an ~10% increase in the Trp53−Cys25-TNB distance, relative to the N state distance. Similarly, the 15% loss of FRET efficiency for Cys62-TNB corresponds to an ~11% increase in the Trp53−Cys62-TNB distance, relative to that in the N state. If the distance of the surface cysteine from the core tryptophan is taken to represent the radius of the protein (assumed to be spherical), then a 10% loss of FRET efficiency corresponds to an ~40% increase in the volume of the protein. It is important, however, to note that this increase in volume may not represent an overall change in volume, because it could be occurring due to expansion of the surface away from the core, without the core itself being significantly solvated.

FRET-Monitored Kinetics for the Buried Acceptors. The loss of FRET efficiency for the Trp53−Cys82-TNB pair occurs in a single phase at a rate similar to the rate of core solvation seen in the unlabeled protein. This implies that the change in the Trp53−Cys82 distance occurs concurrently with core solvation, which is not altogether unexpected because both the donor and acceptor are buried residues. This suggests that the distances within the core change slowly compared to the changes at the surface residues, further supporting the conclusion that structural changes occur slower in the core than on the surface. The unfolding kinetics of this FRET pair also indicate that TNB labeling does not influence the unfolding kinetics of the protein.

The Tyr47−Pro48 bond in barstar is *cis* in the native state, and in the unfolded state it can exist both in the *cis* (U_F or the fast folding form) and *trans* (U_S or the slow folding form) conformations. The U_F and U_S forms are identical except for the conformation of a single proline bond. Normally, the proline isomerization step involving the Tyr47−Pro48 bond can be detected by fluorescence measurement only in the transition zone of unfolding, because it is here that it is coupled kinetically to the structural unfolding reaction during which the change in fluorescence actually occurs. Beyond the transition zone (>5 M urea), the unfolding kinetics are single-exponential (*18*, *27*), because unfolding to the U_F state occurs rapidly and is complete before the subsequent proline isomerization step begins; hence, the two reactions are no longer coupled. The loss of FRET efficiency for the Trp53−Cys40-TNB pair occurs in two phases (Figure 5), both of which are slower than the unfolding rates of the unlabeled protein. The stability of this mutant increases upon TNB labeling (Table 2), and the increased stability may be the reason for the fast unfolding rate being slower for the TNB-labeled protein than for the unlabeled protein. The important information from the FRET-monitored kinetics for this mutant protein is that the slow unfolding rate, which can be observed even at high denaturant concentrations, is independent of denaturant at high urea concentrations (>5 M). Also, the amplitude of this slow phase is not dependent on denaturant concentration beyond the transition zone. The magnitude of this rate is characteristic of the rate of the proline isomerization reaction. It appears that the proline isomerization reaction, which normally cannot be observed by any spectroscopic measurement, can be observed by the measurement of the change in FRET efficiency between Trp53 and Cys40-TNB, because the Tyr47−Pro48 bond is in the middle of this FRET pair in the protein sequence. Thus, the exquisite sensitivity of FRET to small distance changes allows FRET to be exploited in probing the proline isomerization reaction in the unfolded form of the protein, under conditions where the reaction is otherwise silent to all other spectroscopic probes.

Unfolding Pathway of Barstar. It had been shown in earlier unfolding studies that barstar unfolds *via* parallel unfolding pathways with multiple intermediates (*10*−*12*). In light of the FRET experiments discussed here, it appears that the native state expands initially at the surface, while, simultaneously, changes in the secondary structure and core solvation occur at slightly different rates, as the protein unfolds along multiple routes. Theoretical studies have suggested that all protein chains leaving the native state cannot directly access the stable denatured state, but must first surmount one particular energy barrier to reach stable denatured conformations, after which multiple unfolding routes become accessible (*4*).

Surface Expansion and Core Solvation Occur Simultaneously and Not Sequentially. The observation that the loss in FRET efficiency occurs in two kinetic phases for Cys25 and Cys62 (Figure 7) might suggest that unfolding occurs through a mechanism of the N → I → U type, where the intermediate I has a packed core but an overall larger dimension than N. In such a mechanism, the fast change in FRET efficiency would occur during the N → I transition, due to the surface residues moving away from the core. The core solvation and remaining loss of FRET efficiency would then occur during the I → U transition. Such a mechanism would, however, predict that a lag should be observed in the change in core solvation observed by the fluorescence change in the unlabeled protein, but no lag is observed for any of the proteins. Instead of invoking more complex mechanisms, we find it is simpler to assume that core solvation and surface expansion occur simultaneously and independently, but that the latter occurs faster. An analogy may be made to the unfolding of a two-domain protein, where one domain may unfold independently of the other. It is proposed here that the surface of the protein expands faster than, and independent of, core expansion and solvation.

Equilibrium unfolding studies of barstar using the Trp53−Cys82-TNB FRET pair have shown that the protein expands progressively through a continuum of native-like states, and

achieves the dimensions of a molten globule-like state before undergoing a first-order unfolding reaction (*32*). In these expanded native-like states, the secondary structure and core solvation remain as they are in the native state. In the kinetic experiments monitored by FRET here, a surface expansion is seen to occur in a fast phase independent of the core solvation. It is not surprising that this expansion is not seen for the buried residues (Cys82 and Cys40), because the changes in the distances of these residues from the core tryptophan are very likely to occur at a rate similar to the rate of core solvation. The FRET-monitored kinetics therefore provide further evidence in support of the multistate nature of the unfolding reaction of barstar, and provide additional information about how the unfolding structural transition might occur.

Relation of Stability and Structure Formation and/or Loss. Hydrogen exchange (HX) studies which exploit the ability of amide protons in a protein to exchange with solvent protons have been used extensively to characterize the structures and stabilities of various regions of the protein under equilibrium conditions, as well as in kinetic experiments (reviewed in ref *53*). A comparison of the native state HX labeling pattern of oxidized cytochrome *c* (*24*, *54*) and RNase H (*25*, *55*) with pulsed HX labeling experiments on the refolding of the same proteins has indicated that the regions most protected from exchange at equilibrium are the first to acquire structure during refolding.

The packing of amino acid residues in the hydrophobic core of a protein has been shown to have a profound effect on stability and structure (*56*−*58*). It was earlier shown that consolidation of the core occurs before the formation of significant secondary and tertiary structure during the slow refolding reaction of barstar (originating from the U_S molecules) (*41*). These studies demonstrate that thermodynamic stability may govern the kinetics of structure formation. A corollary would be that the least stable regions would be the first to unfold. The FRET-monitored kinetics reported here show that during unfolding, the surface residues move away from the core; that is, partial changes in the tertiary structure occur faster than core solvation. Thus, the gross structural changes that occur during unfolding seem to be the reverse of those that occur during refolding; the core residues, which form a compact state first during refolding, are the residues that are the last to unfold.

HX experiments can be used to probe only those residues which are protected in the native state, either due to hydrogen bonding or due to solvent inaccessibility. Thus, HX studies provide no information about surface amide hydrogens that exchange in both the native and unfolded states. The FRET methodology used here involving surface residues is therefore the first direct experimental observation of the dynamics of the surface during unfolding.

CONCLUSIONS

The unfolding kinetics of barstar, monitored by changes in FRET efficiency for four FRET pairs, indicate that structural changes occur faster at the surface than in the core. It is also shown that FRET efficiency is very sensitive to, and can be utilized to monitor, small structural perturbations such as proline isomerization, under conditions where such measurement is not possible using any other spectroscopic probe. FRET is an effective tool for monitoring fast structural transitions, and appropriate positioning of the FRET pairs has been used to obtain information about specific regions of the protein during unfolding.

ACKNOWLEDGMENT

We thank M. K. Mathew and G. Krishnamoorthy for discussion and useful insights into the interpretation of the data, R. Sowdhamini for the solvent exposure calculation, A. S. R. Koti and G. S. Lakshmikanth for discussion, and R. Sade for obtaining the mass spectra of the proteins.

SUPPORTING INFORMATION AVAILABLE

Representative kinetic trace of unfolding of W38F/W44F in 7.9 M urea at pH 8.0. This material is available free of charge via the Internet at http://pubs.acs.org.

REFERENCES

1. Levinthal, C. (1968) *J. Chem. Phys. 65*, 44−45.
2. Baldwin, R. L. (1995) *J. Biomol. NMR 5*, 103−109.
3. Dill, K. A., and Chan, H. S. (1997) *Nat. Struct. Biol. 4*, 10−19.
4. Dill, K. A., and Chan, H. S. (1998) *Proteins*: *Struct., Funct., Genet. 24*, 2−33.
5. Kiefhaber, T., Labhardt, A. M., and Baldwin, R. L. (1995) *Nature 375*, 513−515.
6. Philips, C. M., Mizutani, Y., and Hochstrasser, R. M. (1995) *Proc. Natl. Acad. Sci. U.S.A. 92*, 7292−7296.
7. Juneja, J., and Udgaonkar, J. B. (2002) *Biochemistry 41*, 2641−2654.
8. Konermann, L., Rosell, F. I., Mauk, A. G., and Douglas, D. J. (1997) *Biochemistry 36*, 6448−6454.
9. Hoeltzli, S. D., and Frieden, C. (1995) *Proc. Natl. Acad. Sci. U.S.A. 92*, 9318−9322.
10. Nath, U., Agashe, V. R., and Udgaonkar, J. B. (1996) *Nat. Struct. Biol. 3*, 920−923.
11. Zaidi, F. N., Nath, U., and Udgaonkar, J. B. (1997) *Nat. Struct. Biol. 4*, 1016−1024.
12. Ramachandran, S., Rami, B. R., and Udgaonkar, J. B. (2000) *J. Mol. Biol. 297*, 733−745.
13. Zocchi, G. (1997) *Proc. Natl. Acad. Sci. U.S.A. 94*, 10647−10651.
14. Oberhauser, A. F., Hansma, P. K., Carrion-Vazquez, M., and Fernandez, J. M. (2001) *Proc. Natl. Acad. Sci. U.S.A. 98*, 468−472.
15. Bryant, Z., Pande, V. S., and Rokhsar, D. S. (2000) *Biophys. J. 78*, 584−589.
16. Leeson, D. T., Gai, F., Rodriguez, H. M., Gregoret, L. M., and Dyer, R. B. (2000) *Proc. Natl. Acad. Sci. U.S.A. 97*, 2527−2532.
17. Sham, Y. Y., Ma, B., Tsai, C. J., and Nussinov, R. (2002) *Proteins 46*, 308−320.
18. Schreiber, G., and Fersht, A. R. (1993) *Biochemistry 32*, 11195−11203.
19. Parker, M. J., and Marqusee, S. (1999) *J. Mol. Biol. 293*, 1195−1210.
20. Forge, V., Wijesinha, R. T., Balbach, J., Brew, K., Robinson, C. V., Redfield, C., and Dobson, C. M. (1999) *J. Mol. Biol. 288*, 673−688.
21. Milne, J. S., Xu, Y., Mayne, L. C., and Englander, S. W. (1999) *J. Mol. Biol. 290*, 811−822.
22. Bachmann, A., and Kiefhaber, T. (2001) *J. Mol. Biol. 306*, 375−386.
23. Plaxco, K. W., Simons, K. T., Ruczinski, I., and Baker, D. (2000) *Biochemistry 39*, 11177−11183.
24. Bai, Y., Sosnick, T. R., Mayne, L., and Englander, S. W. (1995) *Science 269*, 192−197.
25. Chamberlain, A. K., Handel, T. M., and Marqusee, S. (1996) *Nat. Struct. Biol. 3*, 782−787.
26. Bhuyan, A. K., and Udgaonkar, J. B. (1998) *Proteins*: *Struct., Funct., Genet. 30*, 295−308.
27. Sridevi, K., and Udgaonkar, J. B. (2002) *Biochemistry 41*, 1568−1578.
28. Feng, Z., Ha, J.-H., and Loh, S. N. (1999) *Biochemistry 38*, 14433−14439.
29. Wu, P., and Brand, L. (1994) *Anal. Biochem. 218*, 1−13.
30. Selvin, P. R. (2000) *Nat. Struct. Biol. 9*, 730−734.

31. Lakowicz, J. R. (1999) in *Principles of Fluorescence Spectroscopy*, 2nd ed., pp 368−373, Kluwer Academic/Plenum Publishers, Dordrecht, The Netherlands.
32. Lakshmikanth, G. S., Sridevi, K., Krishnamoorthy, G., and Udgaonkar, J. B. (2001) *Nat. Struct. Biol. 8*, 799−804.
33. Navon, A., Ittah, V., Landsman, P., Scheraga, H. A., and Haas, E. (2001) *Biochemistry 40*, 105−118.
34. Lyubovitsky, J. G., Gray, H. B., and Winkler, J. R. (2002) *J. Am. Chem. Soc. 124*, 5481−5485.
35. Lillo, M. P., Beechem, J. M., Szpikowska, B. K., Sherman, M. A., and Mas, M. T. (1997) *Biochemistry 36*, 11261−11272.
36. Tezcan, F. A., Findley, W. M., Crane, B. R., Ross, S. A., Lyubovitsky, J. G., Gray, H. B., and Winkler, J. R. (2002) *Proc. Natl. Acad. Sci. U.S.A. 99*, 8626−8630.
37. Teilum, K., Maki, K., Kragelund, B. B., Poulsen, F. M., and Roder, H. (2002) *Proc. Natl. Acad. Sci. U.S.A. 99*, 9807−9812.
38. Shastry, M. C., Agashe, V. R., and Udgaonkar, J. B. (1994) *Protein Sci. 3*, 1409−1417.
39. Shastry, M. C., and Udgaonkar, J. B. (1995) *J. Mol. Biol. 247*, 1013−1027.
40. Agashe, V. R., Shastry, M. C., and Udgaonkar, J. B. (1995) *Nature 377*, 754−757.
41. Sridevi, K., Juneja, J., Bhuyan, A. K., Krishnamoorthy, G., and Udgaonkar, J. B. (2000) *J. Mol. Biol. 302*, 479−495.
42. Khurana, R., Hate, A. T., Nath, U., and Udgaonkar, J. B. (1995) *Protein Sci. 4*, 1133−1144.
43. Nath, U., and Udgaonkar, J. B. (1997) *Biochemistry 36*, 8602−8610.
44. Ramachandran, S., and Udgaonkar, J. B. (1996) *Biochemistry 35*, 8776−8785.
45. Agashe, V. R., and Udgaonkar, J. B. (1995) *Biochemistry 34*, 3286−3299.
46. Chen, R. F. (1967) *Anal. Lett. 1*, 35−42.
47. Dale, R. E., Eisinger, J., and Blumberg, W. E. (1979) *Biophys. J. 26*, 161−194.
48. Haas, E., Katchalski-Katzir, E., and Steinberg, I. Z. (1978) *Biochemistry 17*, 5064−5070.
49. Swaminathan, R., Nath, U., Udgaonkar, J. B., Periasamy, N., and Krishnamoorthy, G. (1996) *Biochemistry 35*, 9150−9157.
50. Dos Remedios, C. G., and Moens, P. D. J. (1995) *J. Struct. Biol. 115*, 175−185.
51. Lubienski, M. J., Bycroft, M., Freund, S. M., and Fersht, A. R. (1994) *Biochemistry 33*, 8866−8877.
52. Pappu, R. V., Srinivasan, R., and Rose, G. D. (2000) *Proc. Natl. Acad. Sci. U.S.A. 97*, 12565−12570.
53. Englander, S. W. (2000) *Annu. Rev. Biophys. Biomol. Struct. 29*, 213−238.
54. Roder, K., Elove, G. A., and Englander, S. W. (1988) *Nature 335*, 700−704.
55. Raschke, T. M., and Marqusee, S. (1997) *Nat. Struct. Biol. 4*, 298−304.
56. Axe, D. D., Foster, N. W., and Fersht, A. R. (1996) *Proc. Natl. Acad. Sci. U.S.A. 93*, 5590−5594.
57. Munson, M., and Regan, L. (1996) *Protein Sci. 5*, 1584−1593.
58. Reidhaar-Olson, J. F., and Sauer, R. T. (1988) *Science 241*, 53−57.
59. Richards, F. M. (1974) *J. Mol. Biol. 82*, 1−14.

BI0268697